HHS Public Access

Author manuscript

Ophthalmology. Author manuscript; available in PMC 2017 October 01.

Published in final edited form as:

Ophthalmology. 2016 October ; 123(10): 2183–2195. doi:10.1016/j.ophtha.2016.06.048.

Characterization of chorioretinopathy associated with mitochondrial trifunctional protein disorders: Long-term follow-up of 21 cases

Erin A. Boese, MD[1], **Nieraj Jain, MD**[2], **Yali Jia, PhD**[1], **Catie L. Schlechter, MS, CGC**[1], **Cary O. Harding, MD**[3], **Simon S. Gao, PhD**[1], **Rachel C. Patel, BA**[1], **David Huang, MD, PhD**[4], **Richard G. Weleber, MD**[1], **Melanie B. Gillingham, PhD**[3], and **Mark E. Pennesi, MD, PhD**[1]

[1]Oregon Retinal Degeneration Center, Casey Eye Institute, Oregon Health & Science University

[2]Department of Ophthalmology, Emory University

[3]Molecular & Medical Genetics, Oregon Health & Science University

[4]Center for Ophthalmic Optics & Lasers, Oregon Health & Science University

Abstract

Objective—To assess long-term effects of genotype on chorioretinopathy severity in subjects with mitochondrial trifunctional protein (MTP) disorders.

Design—Retrospective case series.

Participants—Consecutive patients with MTP disorders evaluated at a single center from 1994 to 2015, including 18 subjects with long-chain 3-hydroxyacyl-CoA dehydrogenase deficiency (LCHADD) and 3 subjects with trifunctional protein deficiency (TFPD).

Methods—Local records from all visits were reviewed. Every subject underwent complete ophthalmic examination and was evaluated by a metabolic physician and dietitian. Nine subjects underwent ancillary fundoscopic imaging including optical coherence tomography (OCT) and OCT angiography.

Main Outcome Measures—The primary outcome measure was best-corrected visual acuity (logMAR) at the final visit. Secondary outcome measures included spherical equivalent refraction, electroretinogram (ERG) b-wave amplitudes, and qualitative imaging findings.

Results—Subjects were followed for a median of 5.6 years (range 0.3–20.2). The median age of LCHADD subjects at initial and final visits was 2.3 and 11.9 years, while the median age for

Address for Reprints: Mark Pennesi, Ophthalmic Genetics, Casey Eye Institute - Marquam Hill, 3375 SW Terwilliger Blvd, Portland, Oregon 97239-4197.

Conflict of Interest: David Huang has a significant financial interest in Carl Zeiss Meditec. Oregon Health & Science University (OHSU), David Huang, and Yali Jia have a significant financial interest in Optovue, a company that may have a commercial interest in the results of this research and technology. Richard Weleber serves on advisory boards for the Foundation Fighting Blindness. These potential conflicts of interest have been reviewed and managed by Oregon Health & Science University.

TFPD subjects at initial and final visits was 4.7 and 15.5 years. Four long-term survivors over the age of 16 years were included (three subjects with LCHADD and one subject with TFPD).

LCHADD subjects demonstrated a steady decline in visual acuity from an average logMAR of 0.23 (Snellen equivalent 20/34) at baseline to 0.42 (Snellen equivalent 20/53) at the final visit, whereas TFPD patients maintained excellent acuity throughout follow up. Subjects with LCHADD, but not TFPD, showed an increasing myopia with a mean decrease in spherical equivalent refraction of 0.24 diopters per year. Multimodal imaging demonstrated progressive atrophy of the outer retina in LCHADD, often preceded by the formation of outer retinal tubulations and choriocapillaris dropout. ERG findings support the more severe clinical profile of LCHADD subjects compared with TFPD; the function of both rods and cones are diffusely attenuated in LCHADD but within normal limits for TFPD subjects.

Conclusions—Despite improved survival with early diagnosis, medical management, and dietary treatment, subjects with the LCHADD subtype of MTP disorder continue to develop visually disabling chorioretinopathy. Multimodal imaging is most consistent with choriocapillaris loss exceeding photoreceptor loss.

INTRODUCTION

Mitochondrial trifunctional protein (MTP) disorders are rare, recessively inherited conditions of impaired fatty acid metabolism. Affected patients typically present at an early age with episodes of hypoketotic hypoglycemia, cardiomyopathy, rhabdomyolysis, hepatomegaly, and sudden death.[1–5] Early recognition and initiation of treatment including dietary modifications have considerably improved survival, and many patients are now living into adulthood.[6,7] Despite these advances, most patients suffer from progressive and advanced visual disability.[8–12]

MTP disorders result from mutations within the trifunctional protein (TFP), a protein complex that catalyzes three specific enzymatic activities in long-chain fatty acid metabolism: 2–3 Enoyl CoA hydrase, long-chain 3-hydroxyacyl-CoA dehydrogenase (LCHAD), and 3-Ketoacyl-CoA thiolase. LCHAD deficiency (LCHADD, OMIM # 609016) is defined by the presence of the common mutation c.1582G>C in at least one allele of the *HADHA* gene, which yields a normal protein expression of the enzyme complex and a predominant deficiency of LCHAD activity with relative sparing of the other two enzymatic activities. Other mutations within the *HADHA* or *HADHB* genes are associated with decreased protein expression and more uniform deficiency of all three enzymatic activities, yielding so-called multifunctional TFP deficiency (TFPD, OMIM # 609015). Though resulting from a similar disruption in fatty acid metabolism, TFPD has several distinct differences including the absence of liver pathology and a milder ocular phenotype.[1,2,13]

We have previously reported the five-year results of a prospective study correlating medical treatment and dietary patterns with chorioretinopathy progression in MTP disorders, which demonstrated relative retention of retinal function among patients with improved dietary management and lower hydroxyl-acylcarnitines.[6] Subjects from this initial study, affected by either LCHADD or TFPD, are now amongst the longest known survivors with the disease. Here we present long-term findings in 21 subjects with up to 20 years of follow-up,

exploring the effect of genotype on chorioretinopathy severity. We provide an *in vivo* structural assessment of the affected retina with multimodal imaging including optical coherence tomography (OCT), OCT angiography, and fundus autofluorescence (FAF) imaging. Using serial electroretinography (ERG), we also demonstrate corresponding functional changes with time.

METHODS

This is a retrospective case series of all patients seen at the Oregon Health & Science University (OHSU) Casey Eye Institute between 9/20/1994 and 8/18/2015 with a diagnosis of either LCHADD or TFPD. All subjects were followed clinically or participated in various research protocols in the OHSU Department of Molecular and Medical Genetics as detailed previously,[6,7] and 13 of these subjects were previously reported in a prospective, open label study evaluating the effect of diet treatment on chorioretinopathy progression.[6] Diagnosis of LCHADD or TFPD was based on the presence of at least two of three of the following: clinical findings, disease specific acylcarnitine profiles, or enzymatic assays in cultured skin fibroblasts. All subjects underwent molecular testing, which identified two deleterious mutations in the *HADHA* or *HADHB* genes in 18 of the 21 cases.

Institutional Review Board of OHSU approval for both study protocol and consent was obtained, and the study followed the tenets set forth by the Declaration of Helsinki. Each subject's legal guardian provided informed consent for obtaining outside records, and subjects greater than seven years of age gave assent to participate.

Medical Clinical Evaluation

Subjects were evaluated by a biochemical geneticist (COH) at Doernbecher Children's Hospital or at the OHSU Clinical and Translational Research Center as part of routine clinical care or a clinical research study, respectively. Patients were asked to maintain a diet low in long-chain fatty acids (LCFAs) and were supplemented with medium-chain triglycerides (MCTs) in order to minimize oxidation as previously described by Gillingham et al.[7] Medical history and complete physical exam including neurological evaluation were completed. Subjects participating in a research study were asked to complete a 3-day diet record and return the completed record to the investigators (MG) for analysis. Blood samples were collected after an overnight fast and analyzed for plasma acylcarnitines by electrospray tandem mass spectrometry at the Biochemical Genetics Laboratory, Mayo Clinic.[14] Dietary intake was assessed by 24-hour dietary recall for patients evaluated clinically by the metabolic dietitian. Non-fasting blood samples were sent for plasma acylcarnitine analysis as described above.

Ophthalmic Clinical Evaluation

Subjects initially underwent a complete ophthalmic exam with cycloplegic refraction and a full field ERG (ffERG). Best-corrected visual acuity (BCVA) was measured with Snellen testing and converted to logarithm of the minimum angle of resolution (logMAR). Nine subjects had additional imaging including spectral domain OCT imaging (Spectralis, Heidelberg Engineering, Germany), OCT angiography (Avanti RTVue XR, OptoVue, Inc.,

Freemont, CA), and wide field FAF imaging (200Tx, Optos PLC, Freemont, CA) at the discretion of the treating ophthalmologist, often based on the availability of these tests and the patient's ability to cooperate. Severities of chorioretinopathy for first and last documented visits were assessed by a retina specialist (NJ) based on the previously described chorioretinopathy staging system.[12] Fundus images and clinical data were used to stage the chorioretinopathy. For visual acuity and refractive error analysis, our records were supplemented with outside ophthalmology records. Visual fields were obtained on subjects old enough to participate, and included a combination of manual and automated kinetic perimetery (Octopus 101 or Octopus 900, Haag-Streit, Koeniz, Switzerland). Static visual fields were performed using the same perimeter, a radially-designed, centrally-condensed grid containing 164 test location[15], the GATEi strategy[16,17], and a 200ms stimulus of size V on a white background of 10 cd/m^2. The Reliability Factor (RF) for the static perimetry was calculated as the sum of positive and negative catch trials divided by the total number of catch trials presented (designated as a percentage). The sensitivity values were imported into a custom software application (U.S. Patent no 8,657,446 Visual Field Modeling and Analysis (VFMA), OHSU Office of Business and Technology) to model the hill of vision. The volumetric indices (in decibel-steradian or dB-sr) of differential luminance sensitivity, V_{tot}, $V_{30°}$, and V_{periph} (V_{tot} minus $V_{30°}$) and defect space, D_{tot}, $D_{30°}$, and D_{periph} (D_{tot} minus $V_{30°}$), were measured from the model as previously described[15].

En face OCT images of the outer retina and RPE were derived from the mean reflectance of slabs 25 to 45 μm above Bruch's membrane (BM) and 25 μm above BM to BM, respectively. OCT angiography images were derived using the split-spectrum amplitude-decorrelation angiography (SSADA) algorithm.[18,19] The en face OCT angiography of the choroid was the maximum flow projection below BM.

Subjects underwent ffERG testing (custom ERG unit, Casey Eye Institute, Portland, OR) following the standard of the International Society for Clinical Electrophysiology of Vision.[6,20] A previously described locally developed normative database stratified for age and using the identical machine and testing parameters was used in ERG analysis.[6] Most subjects were sedated for ERG testing until eight years of age, and completed unsedated ERG testing at age nine and older.

The primary endpoint was logMAR visual acuity at the final visit. Secondary endpoints included spherical equivalent refraction, ffERG b-wave amplitudes, ffERG b-wave implicit times, and qualitative imaging findings.

Statistical Methods

Baseline sample characteristics were summarized with mean and standard deviations (SD) for continuous variables, and frequencies and percentages for categorical variables. Snellen best corrected visual acuities were converted to logMAR values for analysis. Visual acuities of count fingers were first converted to Snellen acuities based on the assumption that fingers are approximately the size of a "200 letter."[21] Some patients were too young to perform Snellen acuity testing; those visits were not included within the analysis. In all instances, these were measured as "central, steady, and maintained" and did not differ among subjects.

For analysis of visual acuity over time, only subjects with two or more recorded Snellen acuities were included.

Correlation between age and visual acuity (logMAR) for subjects with LCHADD and subjects with TFPD were calculated using a Pearson correlation for data sets that were normally distributed and Spearman correlation for data sets that were non-normally distributed. The linear fit of the visual acuity versus age was compared between subjects with LCHADD and subjects with TFPD to determine if the slope or intercept of the line was significantly different between groups. For ERG results, OD/OS values were averaged and all data points expressed as absolute value compared to age and testing conditions (sedated versus unsedated, Figure 3) and expressed as a z-score (value – mean/SD) for that age and testing condition. For all subjects with 4 or more ERG measurements, we compared the change over time z-scores between groups with a repeated measures ANOVA. Prism 6.0 software (Graphpad, Inc. La Jolla, CA) was used for all analyses and $p< 0.05$ was considered statistically significant.

RESULTS

Twenty-one subjects were followed for a median of 5.6 years (7.0 years for LCHADD, range 0.3–20.2; 5.3 years for TFPD, range 5.2–14.7) (Table 1). Median age for LCHADD subjects at the initial and final visits was 2.3 (range 0.4–17.7) and 11.9 (range 3.3–24.2) years, and median age for TFPD subjects at the initial and final visits was 4.7 (range 1.0–10.3) and 15.5 (6.3–19.4) years respectively. Nine of the 16 LCHADD patients, and two of three TFPD patients, were older than 12 years at the final visit. All LCHADD patients were diagnosed within the first nine months of life (range birth–9 months), and all TFPD patients were diagnosed by early childhood (range birth-3 years). Of note, many patients did not undergo ophthalmic examination immediately upon diagnosis. During the course of the study, two LCHADD subjects and one TFPD subject died from cardiac complications.

Patient Characteristics

Eighteen of the 21 patients were diagnosed with LCHADD, characterized by the presence of the common mutation (c.1582G>C) in at least one allele of the *HADHA* gene. Of these, nine (50%) were homozygous, and six (33%) were characterized as compound heterozygotes, containing a variety of known pathogenic mutations as well as novel mutations predicted to be pathogenic. A second mutation was not isolated in three (16.7%) subjects (Table 1).

Of the three subjects with a clinical diagnosis of TFPD, each had the c.901G>A mutation within the *HADHB* gene, although the second mutation was not identified in any case (Table 1). Two of the three subjects were siblings, and presumably had the same causative mutations.

Subjects presented symptomatically with hypoketotic hypoglycemia, rhabdomyolysis or were identified pre-symptomatically due to the diagnosis of an older sibling (Table 1). All subjects and/or their guardians were counseled to avoid fasting, follow a low long-chain fat diet, and consume medium-chain triglyceride (MCT) supplements. Some subjects were prescribed oral carnitine supplements. All subjects had at least one hospital admission for

rhabdomyolysis consistent with metabolic decompensation of LCHAD and TFP deficiencies. Subjects consumed approximately 10–17% of total energy from long chain fat and 10–20% of energy from MCT supplements based on available diet recall analysis (Supplemental Table 1, available at http://aaojournal.org).[6,7] A sum of all the plasma long-chain hydroxyl-acylcarnitine species was calculated. Low metabolite concentrations of <1.5 μmol/L were observed in 11 subjects, including all 3 subjects with TFPD. High metabolite concentrations of >1.5 μmol/L were observed in 5 subjects with LCHADD.

Visual Acuity

Visual acuity progression was assessed using the mean logMAR between the two eyes at each visit. In subjects with LCHADD, mean baseline and final BCVA was 0.23 ± 0.26 and 0.42 ±0.31 (Snellen equivalent 20/34 and 20/53), respectively. The correlation between age and decrease in logMAR was significant for subjects with LCHADD but not for subjects with TFPD (Spearman r=0.88; p<0.001 LCHADD; r= −0.5, p=0.79 TFPD). Taking all BCVA values together, grouped by age, there was a linear decline with slope of approximately 0.034 logMAR units per year among patients with LCHADD (R^2=0.66) not observed among patients with TFPD (Figure 1A). There was also a notable disparity between the eyes of LCHADD subjects. The overwhelming majority (16 of 18 LCHADD patients) retained a final logMAR visual acuity of 0.3 (20/40) or better in one eye despite a decline with advancing age in the other (Figure 1B; Pearson r=0.85 p<0.0001). The other two patients had very advanced disease; on the final visit, LC02 had visual acuities of 0.8 and 0.7, and LC13 had visual acuities of 1.0 and 0.7 at ages 15.8 and 9.8 years respectively. Subjects with TFPD all had excellent and stable visual acuity, with mean final logMAR 0.02 ± 0.03 (Snellen equivalent 20/21) (Figure 1A).

Many subjects were too young for the majority of the study to reliably perform visual field testing. Six LCHADD subjects and one TFPD subject had at least one visual field during the course of the study, and a total of three LCHADD subjects underwent more than one visual field. LC14 had a series of visual fields performed over 9.5 years (Supplemental Figures 1–3, available at http://aaojournal.org), which demonstrated a progression consistent with prior studies.[11] On kinetic perimetry, this patient had small bilateral paracentral scotomata in each eye on initial testing early in the disease, and with time, these paracentral defects enlarged and deepened (Supplemental Figure 1, available at http://aaojournal.org). Static testing at 24.2 years of age disclosed a profoundly decreased foveal sensitivity of 14.5 dB (normal 37.4 dB) and a small ring scotoma within 10° of fix ation in the right eye (Supplemental Figure 2, available at http://aaojournal.org). For the left eye, the sensitivity at foveal fixation was 29.2 dB and located on the temporal size of a small, irregular shaped 23.9 deg^2 region of sensitivity just nasal to fixation that peaked at 32.4 dB. When viewed in defect space, this small region of preserved field remained throughout its extent within 7.6 dB of normal expected sensitivity (Supplemental Figure 3, available at http://aaojournal.org).

Refractive Error

Subjects with LCHADD had progressive myopia with a mean decline in spherical equivalent of −0.24 diopters per year following a linear trajectory (Spearman correlation between diopters and age r = −0.82; p<0.001; Figure 2). Unlike typical myopic progression that

stabilizes by teenage years, patients with LCHADD had a steady myopic decline that continued into early adulthood. Many patients developed high myopia by their teenage years. In contrast to BCVA, there was minimal disparity in refractive error between the eyes of individual subjects. Subjects with TFPD did not develop a significant myopic shift (Figure 2). There was a significant difference in the slope of the linear fit between subjects with LCHADD and subjects with TFPD (Linear regression slope for LCHAD = −0.24; slope for TFP −0.036, difference $p < 0.033$).

Electroretinography

Subjects with LCHADD developed diffusely attenuated ERG amplitudes with prolonged implicit times at an early age, while TFPD patients maintained normal ERG responses (Figure 3). Change over time was greater among subjects with LCHADD compared to subjects with TFPD for all ERG parameters (repeated measures ANOVA $p < 0.05$ for group differences). LCHADD was associated with lower scotopic and photopic b-wave amplitudes (Figure 3, Supplemental Table 2 available at http://aaojournal.org for specific values), suggesting that both rods and cones are affected in this disease. These ERG changes were seen as early as age 6, often followed by increased rate of decline (Figure 3).

Posterior Segment Findings

The fundus of subjects with LCHADD exhibited a characteristic sequence of changes (Figure 4A). Early in disease, there is macular pigment clumping, followed by a progressive patchy chorioretinal atrophy that starts at the macula, with relative foveal sparing, and extends peripherally. Three subjects with advanced disease developed a hyperpigmented foveal scar (Table 2). TFPD patients maintain a normal funduscopic appearance (Figure 4B).

Posterior Segment Imaging

Fundus autofluorescence imaging in LCHADD patients demonstrated patchy areas of hypoautoflorescence with intervening bridges of intact autofluorescence, suggestive of a sparse reticular network of relatively preserved RPE (Figure 5).

On SD-OCT imaging, early LCHADD disease shows irregularity of the interdigitation zone (IZ) outside of the fovea (Figure 6). With time, there is patchy loss of EZ and subjacent RPE. Regions of tissue loss have abrupt transition between healthy and diseased tissue. At this margin of atrophy, many eyes also have a notable scrolling of outer retinal elements and outer retinal tubulations (ORTs). Three eyes with advanced chorioretinopathy had subfoveal hyperreflective material consistent with scar formation. OCT images were not available in TFPD subjects for comparison.

Two patients with LCHADD chorioretinopathy underwent OCT angiography imaging (Figure 7). One patient is heterozygous for the LCHADD common mutation, and is the oldest patient with longest follow up in our cohort. The other patient is homozygous for the common mutation, and although younger, has advanced disease. OCT angiography demonstrates marked loss of choriocapillaris that was far more extensive than photoreceptor loss as assessed by EZ integrity (Figure 7). Co-registered FAF imaging demonstrated corresponding RPE loss, although due to low signal it was difficult to reliably compare

extent of RPE loss to choriocapillaris loss. No TFPD subjects underwent OCT angiography imaging.

DISCUSSION

LCHADD, but not TFPD, continues to cause progressive chorioretinopathy and myopia despite modern medical and dietary interventions to manage systemic comorbidity. The chorioretinopathy begins with changes that are mostly within the macula and posterior pole, which create paracentral scotomas on static and kinetic testing that enlarge, deepen, and coalesce with time. As demonstrated on the static visual fields, the pathology is weighted toward the center portion of the field, but does not have the consistent radial or bilateral symmetry seen in most forms of retinitis pigmentosa.[22] Although the variability may be influenced by diet, some of the variability may relate to stochastic events. Our findings on in vivo SD-OCT and OCT angiography analysis, derived from the largest series on MTP disorder-associated chorioretinopathy with some of the oldest known subjects, suggest once again that photoreceptor degeneration may be secondary to an insult in either the RPE or choriocapillaris. These tissue layers may be optimal targets for future treatment approaches.

Structural assessment with *en face* multimodal imaging including OCT angiography demonstrates that RPE and choriocapillaris loss is more extensive than photoreceptor loss (Figure 7) in subjects with LCHADD. Furthermore, the outer retina was noted to scroll at the margins of degeneration with formation of ORTs (Figure 6). ORTs have been noted in a number of degenerative conditions of the RPE and choriocapillaris, including geographic atrophy and choroideremia.[23,24] A prevailing theory is that photoreceptors form ORTs as a survival strategy in the context of loss of trophic support from a degenerating RPE or choriocapillaris.[25]

In general, visual field loss in LCHADD correlates well with the anatomic changes seen in the disease. In studying the relationship between outer retina structure and field changes in retinitis pigmentosa, Travis et al. found that areas of absent EZ correlated well with areas of sensitivity 7.6dB below normal or less. A similar structure-function correlation was found in LCHADD subject LC14; the left eye at 24.2 years of age had preservation of a region of field where the sensitivity defect was less than 7.6 dB. Furthermore, in that same eye, ORTs were present in the retina just temporal to the fovea (Figure 6C), which corresponded to the region of retained sensitivity just nasal to fixation in the static visual field (Supplemental Figure 2, available at http://aaojournal.org). This finding is consistent with the theory ORT formation being an adaptive mechanism that helps preserve retinal function.

Our findings of early RPE degeneration provide *in vivo* corroboration of prior findings from histopathology and cell culture studies. Two post mortem specimens from eyes with LCHADD chorioretinopathy demonstrated macrophage infiltration of the RPE.[8] More recently, a study of patient-specific induced pluripotent stem cell-derived RPE cells containing the LCHAD mutation demonstrated that these cells were smaller, more irregular in shape, and were held together by disorganized tight junctions as compared to normal RPE cells in culture. The affected cells had fewer melanosomes, an increased number of melanolysosomes, and a pathologic accumulation of lipid.[26] In addition to substantiating

these findings, our *in vivo* assessment with OCT angiography allows for longitudinal evaluation of eyes with better preservation of tissue architecture.

Wide-field FAF imaging has proven to be a valuable clinical tool to characterize the extent of degeneration in affected eyes. These images highlight the initial posterior involvement with relative foveal sparing (Figure 5). Subsequent degeneration in the midperiphery, with large scalloped regions of atrophy with an intervening network of relatively preserved RPE, is somewhat reminiscent of other chorioretinopathies such as gyrate atrophy and choroideremia.

Interestingly, despite the early degeneration in the posterior pole, subjects tended to retain good central acuity in at least one eye. Subjects with profound central vision loss frequently exhibited elevated pigmented subfoveal scars. Without histopathologic correlation, the exact nature of this hyperpigmented scar remains uncertain. OCT imaging in one subject demonstrated a subfoveal scar adjacent to a large break in Bruch's membrane suggestive of a prior choroidal neovascularization membrane (CNVM). Alternatively, this pigmented lesion may result from accumulation of inwardly migrating, diseased RPE cells from surrounding tissue; or an idiopathic gliosis. Two prior reports described the development of a similar subfoveal scar,[27,28] one with an active CNVM.[20] Although we did not detect any active CNVM, the finding of a subfoveal scar in 17% of our patients calls for close monitoring of central acuity in affected eyes, perhaps with Amsler grid testing. Acutely symptomatic patients should be promptly evaluated for consideration of anti-vascular endothelial growth factor treatment. Previously, posterior staphyloma has been suggested as the cause of vision loss in patients with LCHADD[11]. Due to the rarity of the disease, a meta-analysis of visual function and chorioretinopathy within long-term survivors would be helpful to better elucidate the frequency of these findings and cause of visual dysfunction.

The lengthy follow-up in this study highlights that progressive myopia in LCHADD continues into adulthood. It is unclear if high axial myopia may represent a comorbid condition with associated degenerative changes, perhaps contributing to CNVM formation. No subjects developed peripheral retinal pathology such as lattice degeneration or retinal tears.

Despite affecting the same enzyme complex, LCHADD and TFPD are two distinct clinical entities with highly disparate ophthalmic findings. Patients with LCHADD have a greater accumulation of potentially toxic metabolites produced by selective loss of LCHAD function with relative preservation of the long-chain hydratase activity compared to relatively low concentrations of metabolites among patients with TFPD and loss of all 3 enzymatic functions.[29] The theory that toxic metabolites are part of the underlying etiology of chorioretinopathy in LCHADD is supported by studies linking low serum 3-hydroxyacylcarnitines and fatty acid byproducts to a milder ophthalmic phenotype, even among patients with the same genotype.[6] A competing theory suggests that the mutated subunit of LCHADD induces retinal cell death by a dominant negative mechanism, possibly through interference of nearby enzymes.[10,29,30] Further research is needed to determine the cause of these disparate ophthalmic phenotypes among patients with mutations in the same enzyme complex.

This study does have limitations. Due to the retrospective study design in this exceedingly rare condition, follow-up is variable with an evolving imaging workup over the course of the study. For instance, evaluation with the novel OCT angiography technology was only performed on two subjects. Second, there are several patients where the modern molecular testing techniques have failed to identify two deleterious mutations, possibly due to pathogenic intronic or splice-site variants. However, the diagnosis has been established in each subject through robust clinical assessment and enzymatic assays of cultured skin fibroblasts. Lastly, dietary intake and metabolic control was assessed at a moment in time but both factors are dynamic, changing from day to day and from moment to moment. There was no way to determine all of the metabolic decompensation episodes in our patients followed in multiple clinics around the US.

CONCLUSIONS

To our knowledge, this is the largest series demonstrating the ophthalmic manifestations of MTP disorders and this series has the longest follow up. With some of the oldest living patients with these diseases, our study provides greater understanding of the clinical progression of these metabolic diseases in the era of improved dietary and metabolic control. Advanced imaging techniques have provided some of the first *in vivo* evidence suggesting that photoreceptor damage may be secondary to atrophy of the RPE and/or choriocapillaris. This finding suggests that the RPE or choriocapillaris may be optimal target tissues for prospective treatments, such as gene therapy. Our series also helps to provide prognostic information to patients; we show that patients with TFPD have minimal clinical and functional retinal changes, while LCHADD patients often progress despite continued medical and dietary treatment.

Supplementary Material

Refer to Web version on PubMed Central for supplementary material.

Acknowledgments

Financial Support: Unrestricted departmental funding from Research to Prevent Blindness, New York, NY (all) Foundation Fighting Blindness (ECDA to MEP, CDA to NJ CF-CL-0614-0647-OHSU) FFB Research Center Grant, Columbia, MD, FFB CDA (CF-CL-0614-0647-OHSU) (RGW) National Eye Institute, Bethesda, MD, P30 EY010572 (all), RO1 EY023285 (DH), RO1 EY024544 (YJ), DP3 DK104397 (YJ)

Clinical and Translational Science Award Grant, Bethesda, MD, UL1TR000128 (YJ, DH)

The sponsor or funding organization had no role in the design or conduct of this research.

Acronyms

BCVA	best-corrected visual acuity
BM	Bruch’s membrane
CNVM	choroidal neovascular membrane
CSM	central, steady, and maintained

ERG	electroretinogram
EZ	ellipsoid zone
ffERG	full field ERG
FAF	fundus autofluorescence
IZ	interdigitation zone
logMAR	logarithm of the minimal angle of resolution
LCFA	long-chain fatty acid, LCHADD, long-chain 3-hydroxyacyl-CoA dehydrogenase deficiency
MCT	medium-chain triglyceride
MTP	mitochondrial trifunctional protein
MTPD	mitochondrial trifunctional protein deficiency
OCT	optical coherence tomography
OHSU	Oregon Health & Science University
ORT	outer retinal tubulation
RPE	retinal pigment epithelium
TFP	trifunctional protein
TFPD	trifunctional protein deficiency
WNL	within normal limits

CITATIONS

1. Wanders RJ, IJlst L, van Gennip AH, et al. Long-chain 3-hydroxyacyl-CoA dehydrogenase deficiency: identification of a new inborn error of mitochondrial fatty acid beta-oxidation. J Inherit Metab Dis. 1990; 13:311–314. [PubMed: 2122092]
2. Rinaldo P, Matern D, Bennett MJ. Fatty acid oxidation disorders. Annu Rev Physiol. 2002; 64:477–502. [PubMed: 11826276]
3. Tyni T, Pihko H. Long-chain 3-hydroxyacyl-CoA dehydrogenase deficiency. Acta Paediatr. 1999; 88:237–245. [PubMed: 10229030]
4. Przyrembel H, Jakobs C, IJlst L, et al. Long-chain 3-hydroxyacyl-CoA dehydrogenase deficiency. J Inherit Metab Dis. 1991; 14:674–680. [PubMed: 1779613]
5. Boer den MEJ, Wanders RJA, Morris AAM, et al. Long-chain 3-hydroxyacyl-CoA dehydrogenase deficiency: clinical presentation and follow-up of 50 patients. Pediatrics. 2002; 109:99–104. [PubMed: 11773547]
6. Gillingham MB, Weleber RG, Neuringer M, et al. Effect of optimal dietary therapy upon visual function in children with long-chain 3-hydroxyacyl CoA dehydrogenase and trifunctional protein deficiency. Molecular Genetics and Metabolism. 2005; 86:124–133. [PubMed: 16040264]
7. Gillingham M. Optimal dietary therapy of long-chain 3-hydroxyacyl-CoA dehydrogenase deficiency. Molecular Genetics and Metabolism. 2003; 79:114–123. [PubMed: 12809642]

8. Tyni T, Pihko H, Kivelä T. Ophthalmic pathology in long-chain 3-hydroxyacyl-CoA dehydrogenase deficiency caused by the G1528C mutation. Current Eye Research. 1998; 17:551–559. [PubMed: 9663844]
9. Bertini E, Dionisi-Vici C, Garavaglia B, et al. Peripheral sensory-motor polyneuropathy, pigmentary retinopathy, and fatal cardiomyopathy in long-chain 3-hydroxy-acyl-CoA dehydrogenase deficiency. Eur J Pediatr. 1992; 151:121–126. [PubMed: 1537353]
10. Fletcher AL, Pennesi ME, Harding CO, et al. Observations regarding retinopathy in mitochondrial trifunctional protein deficiencies. Molecular Genetics and Metabolism. 2012; 106:18–24. [PubMed: 22459206]
11. Tyni T, Kivelä T, Lappi M, et al. Ophthalmologic findings in long-chain 3-hydroxyacyl-Coa dehydrogenase deficiency caused by the G1528C mutation. Ophthalmology. 1998; 105:810–824. [PubMed: 9593380]
12. Tyni T, Immonen T, Lindahl P, et al. Refined Staging for Chorioretinopathy in Long-Chain 3-Hydroxyacyl Coenzyme A Dehydrogenase Deficiency. Ophthalmic Research. 2012; 48:75–81. [PubMed: 22473002]
13. Pons R, Roig M, Riudor E, et al. The clinical spectrum of long-chain 3-hydroxyacyl-CoA dehydrogenase deficiency. Pediatr Neurol. 1996; 14:236–243. [PubMed: 8736409]
14. Smith, EH.; Matern, D. Acylcarnitine Analysis by Tandem Mass Spectrometry. Hoboken, NJ, USA: John Wiley & Sons, Inc; 2001. p. 17.8.1-17.8.20.
15. Weleber RG, Smith TB, Peters D, et al. VFMA: Topographic Analysis of Sensitivity Data From Full-Field Static Perimetry. Transl Vis Sci Technol. 2015; 4:14. [PubMed: 25938002]
16. Schiefer U, Pascual JP, Edmunds B, et al. Comparison of the new perimetric GATE strategy with conventional full-threshold and SITA standard strategies. Invest Ophthalmol Vis Sci. 2009; 50:488–494. [PubMed: 19060285]
17. Luithardt AF, Meisner C, Monhart M, et al. Validation of a new static perimetric thresholding strategy (GATE). Br J Ophthalmol. 2015; 99:11–15. [PubMed: 25053761]
18. Jia Y, Tan O, Tokayer J, et al. Split-spectrum amplitude-decorrelation angiography with optical coherence tomography. Optics Express. 2012; 20:4710–4725. [PubMed: 22418228]
19. Gao SS, Liu G, Huang D, Jia Y. Optimization of the split-spectrum amplitude-decorrelation angiography algorithm on a spectral optical coherence tomography system. Optics Letters. 2015; 40:2305–2308. [PubMed: 26393725]
20. McCulloch DL, Marmor MF, Brigell MG, et al. ISCEV Standard for full-field clinical electroretinography (2015 update). Doc Ophthalmol. 2015; 130:1–12. [PubMed: 25502644]
21. Holladay JT. Visual acuity measurements. J Cataract Refract Surg. 2004; 30:287–290. [PubMed: 15030802]
22. Massof RW, Finkelstein D, Starr SJ, et al. Bilateral symmetry of vision disorders in typical retinitis pigmentosa. Br J Ophthalmol. 1979; 63:90–96. [PubMed: 311654]
23. Goldberg NR, Greenberg JP, Laud K, et al. Outer retinal tubulation in degenerative retinal disorders. Retina (Philadelphia, Pa). 2013; 33:1871–1876.
24. Jain N, Jia Y, Gao SS, et al. Optical Coherence Tomography Angiography in Choroideremia: Correlating Choriocapillaris Loss With Overlying Degeneration. JAMA Ophthalmol. 2016
25. Ma N, Streilein JW. Contribution of microglia as passenger leukocytes to the fate of intraocular neuronal retinal grafts. Invest Ophthalmol Vis Sci. 1998; 39:2384–2393. [PubMed: 9804147]
26. Polinati PP, Ilmarinen T, Trokovic R, et al. Patient-Specific Induced Pluripotent Stem Cell-Derived RPE Cells: Understanding the Pathogenesis of Retinopathy in Long-Chain 3-Hydroxyacyl-CoA Dehydrogenase Deficiency. Invest Ophthalmol Vis Sci. 2015; 56:3371–3382. [PubMed: 26024122]
27. Fahnehjelm KT, Holmström G, Ying L, et al. Ocular characteristics in 10 children with long-chain 3-hydroxyacyl-CoA dehydrogenase deficiency: a cross-sectional study with long-term follow-up. Acta Ophthalmologica. 2007; 86:329–337. [PubMed: 18162058]
28. Stopek D, Gitteau Lala E, Labarthe F, et al. Long-chain 3-hydroxyacyl CoA dehydrogenase deficiency and choroidal neovascularization. J Fr Ophtalmol. 2008; 31:993–998. [PubMed: 19107076]
29. Spiekerkoetter U, Khuchua Z, Yue Z, et al. General mitochondrial trifunctional protein (TFP) deficiency as a result of either alpha- or beta-subunit mutations exhibits similar phenotypes

because mutations in either subunit alter TFP complex expression and subunit turnover. Pediatr Res. 2004; 55:190–196. [PubMed: 14630990]

30. Wang Y, Mohsen A-W, Mihalik SJ, et al. Evidence for physical association of mitochondrial fatty acid oxidation and oxidative phosphorylation complexes. J Biol Chem. 2010; 285:29834–29841. [PubMed: 20663895]

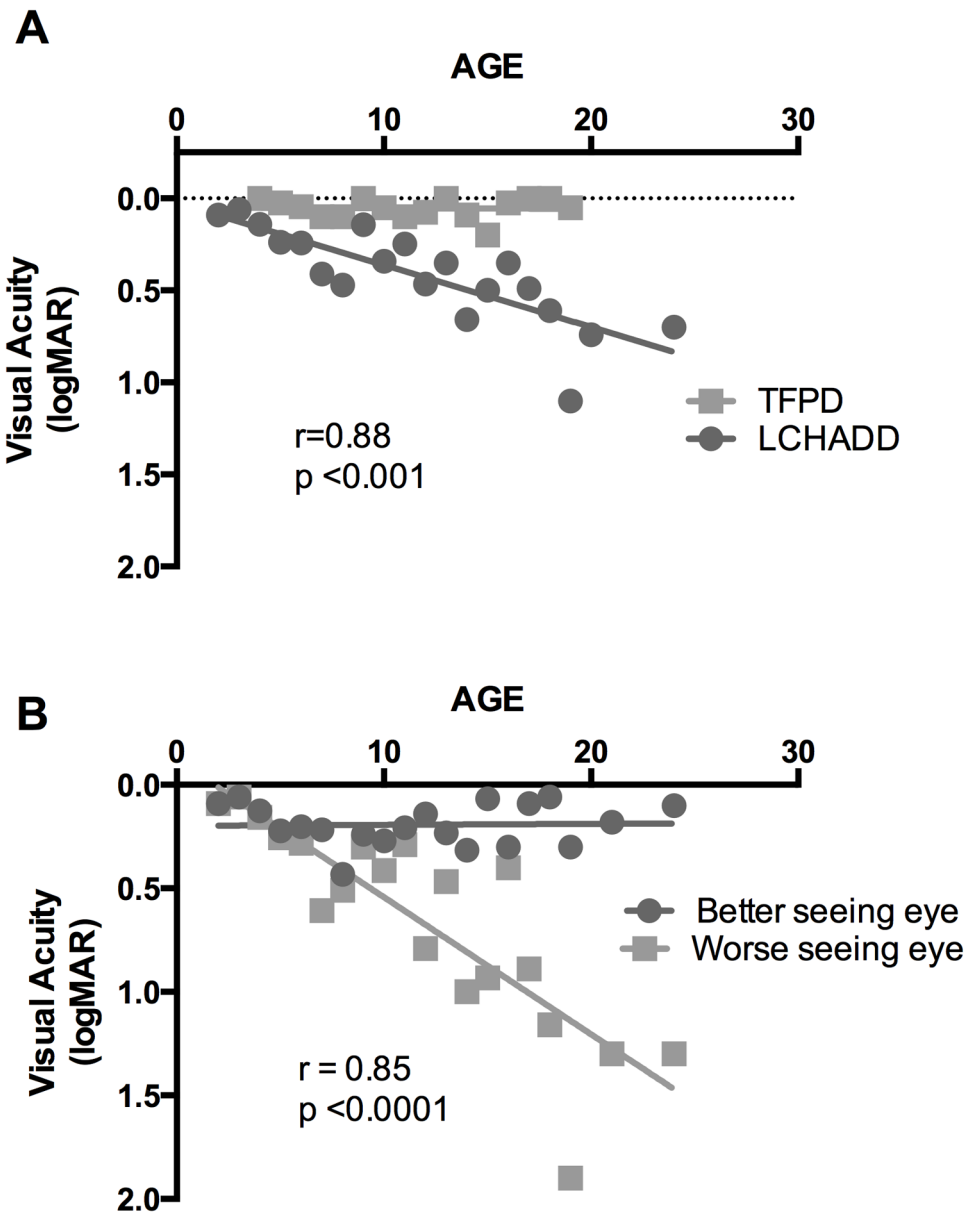

Figure 1. Visual acuity declines in LCHADD eyes but not TFPD eyes

(A) Subjects with LCHADD (circles) had a progressive decline in best-corrected visual acuity with increasing age when all visits of all patients were averaged for each age rounded to nearest year, averaging 0.03 loss of logMAR acuity per year. The data was non-normally distributed. Spearman correlation between logMAR and age was significant ($r=0.88$, $p<0.001$). TFPD patients (squares) maintained excellent visual acuity throughout the study. There was no significant correlation between logMAR and age among subjects with TFPD. **(B) Best-corrected visual acuity plotted individually for the better (circles) and worse seeing (squares) eye in LCHADD patients.** There was a significant correlation between logMAR and age for the worse seeing eye among subjects with LCHADD (Pearson $r= 0.85$; $p<0.0001$).

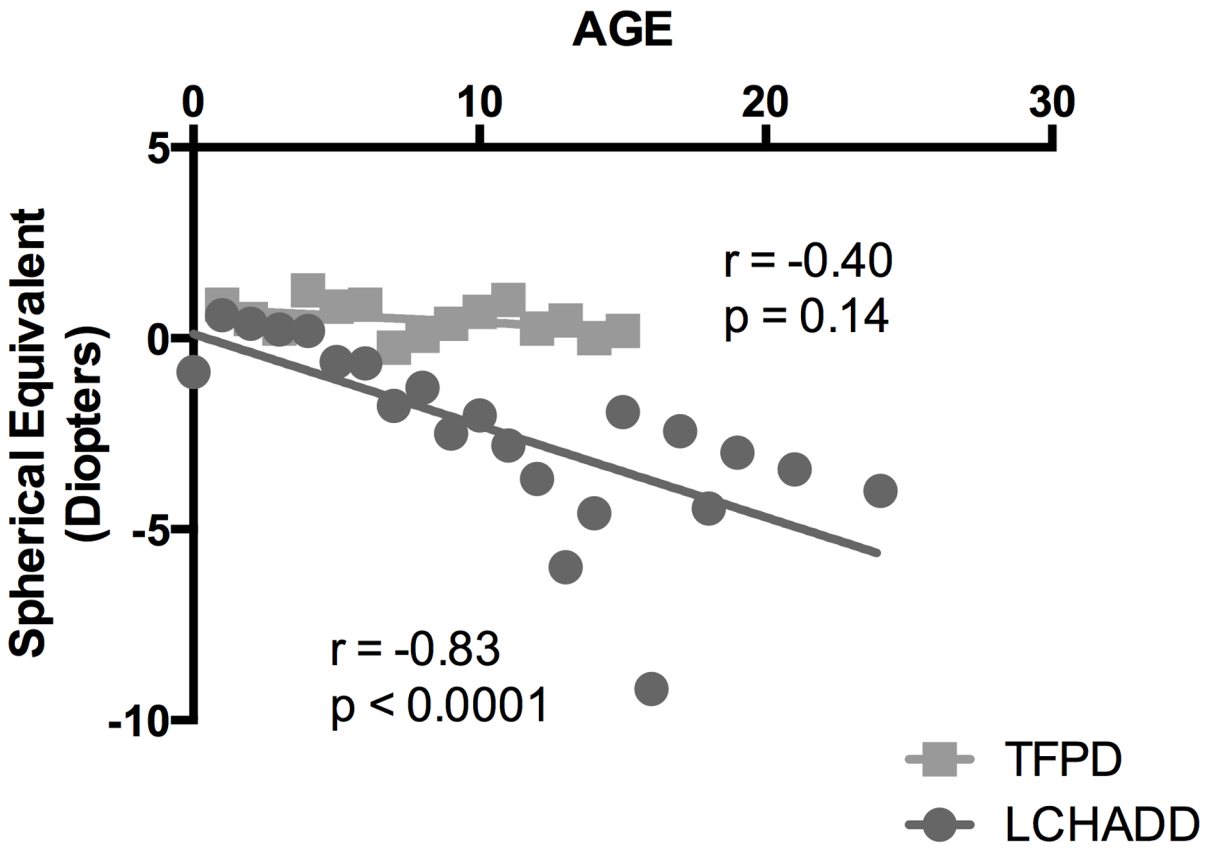

Figure 2. LCHADD subjects have progressive myopia

Subjects with LCHADD had a significant mean decrease in spherical equivalent with increasing age, averaging 0.24 increase in myopia per year when visits of all patients were averaged for age rounded to nearest year. Conversely, subjects with TFPD had minimal progression of myopia, with spherical equivalent decreasing by 0.03 per year. The data was non-normally distributed. Spearman correlation of diopters and age was significant for subjects with LCHAD deficiency ($r=-0.83$, $p<0.0001$) but was not significantly correlated for subjects with TFPD ($p = 0.14$).

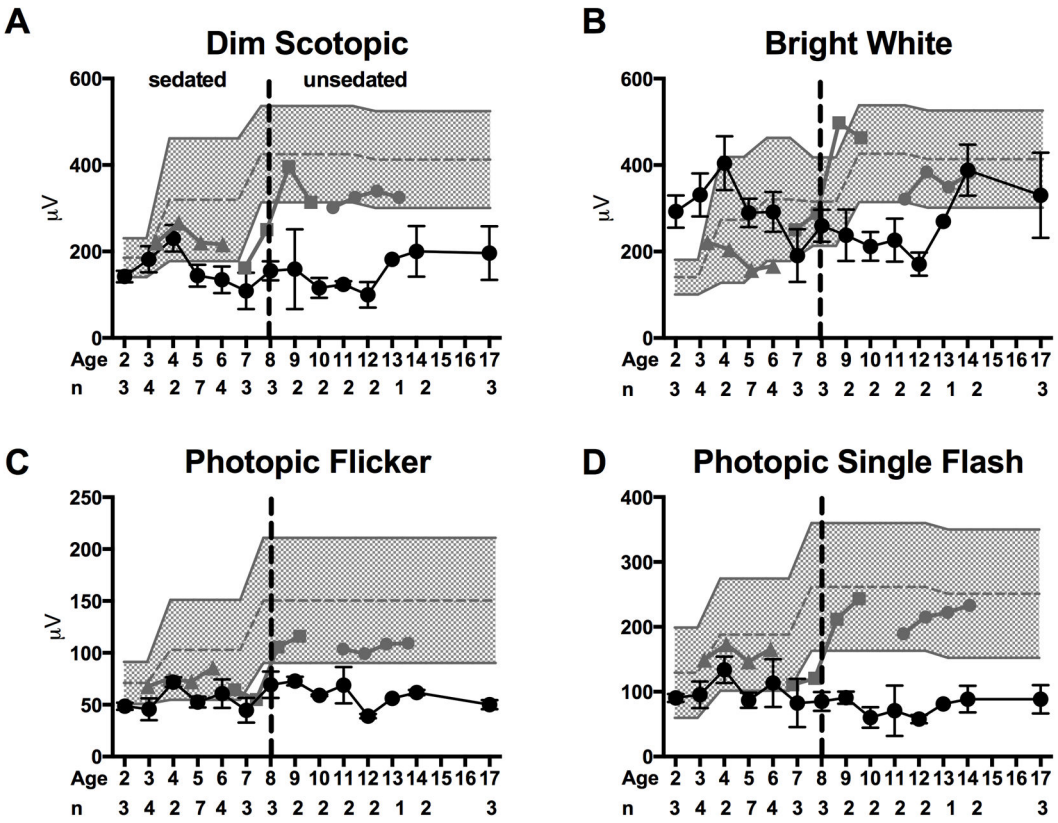

Figure 3. Electroretinogram Mean ± SEM of the

(A) dim scotopic flash b-wave amplitude, (B) bright scotopic flash b-wave amplitude, (C) 30 Hz photopic flicker amplitude, and (D) photopic single flash b-wave amplitude in two groups of subjects by age. The subjects were divided into those with LCHADD (black circle; n for each age given below x-axis) and those with TFPD (n=1 subject at each age; grey triangle= LC18; gray square LC17, grey circle LC16). The normal range of values for each age is shown by gray shading. Subjects were sedated for the test up to age 8 and performed the test awake thereafter. The dashed line demarcates sedated and unsedated values. The presence of one allele of c.1528G>C was associated with lower dim and bright scotopic amplitudes as well as lower photopic and photopic single flash amplitudes.

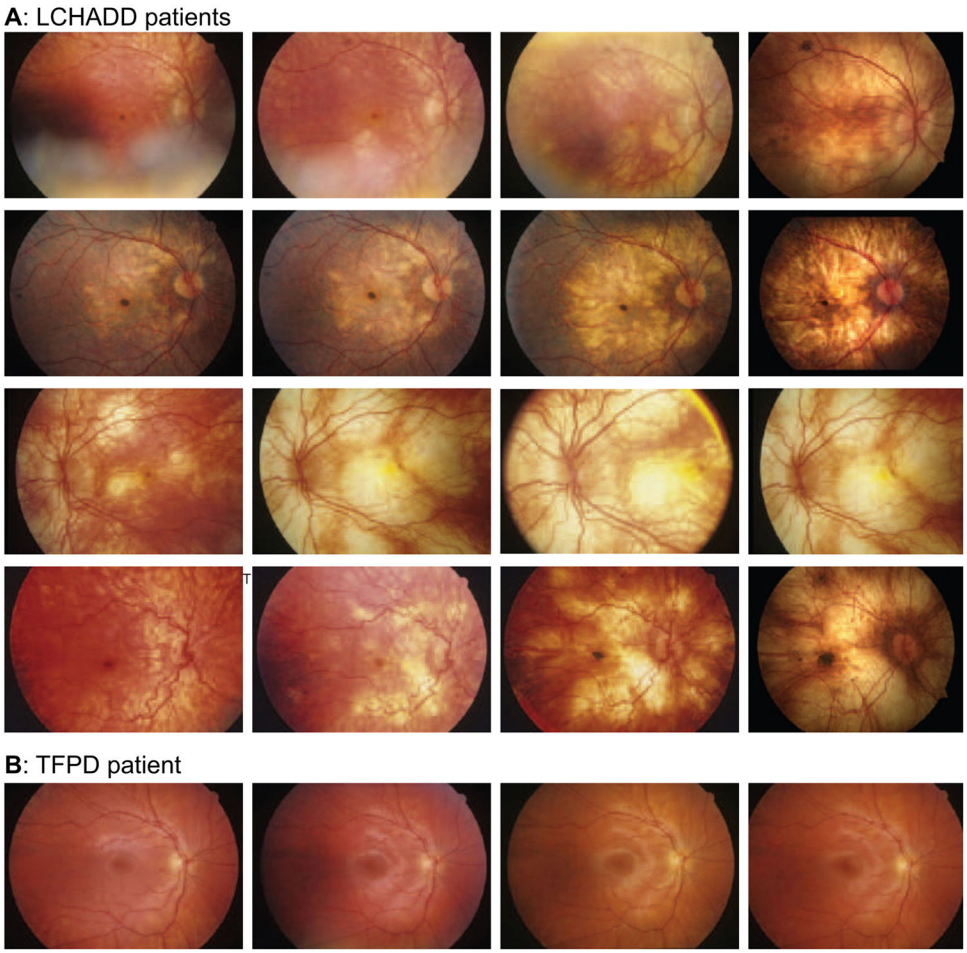

Figure 4.

(A) Color fundus photos demonstrate disease progression despite dietary modification and systemic disease control in several patients with LCHADD. Supratitles in each row indicate the patient and identified genetic mutations. Early in the disease, there is an accumulation of pigment at the central macula, which is followed by a progressive patchy chorioretinal atrophy of the posterior pole. With time, the atrophy extends to involve the periphery. In some subjects, there is relative sparing of peripapillary retina. Late stages of the disease show the development of a subfoveal pigmentary scar (not in all patients). There is minimal retinal vascular attenuation or disc pallor. **(B) Color fundus photos demonstrate disease stability in one patient with TFPD.** Supratitles indicate the patient and identified genetic mutations. Unlike the LCHADD patients, subjects with TFPD did not have any evidence of pigment clumping or chorioretinal atrophy. The fundus photos of subject LC16 remained normal over 4.1 years of photographic follow up. Although not included within the figure, the remaining two subjects with TFPD also did not have any notable changes on fundus photography.

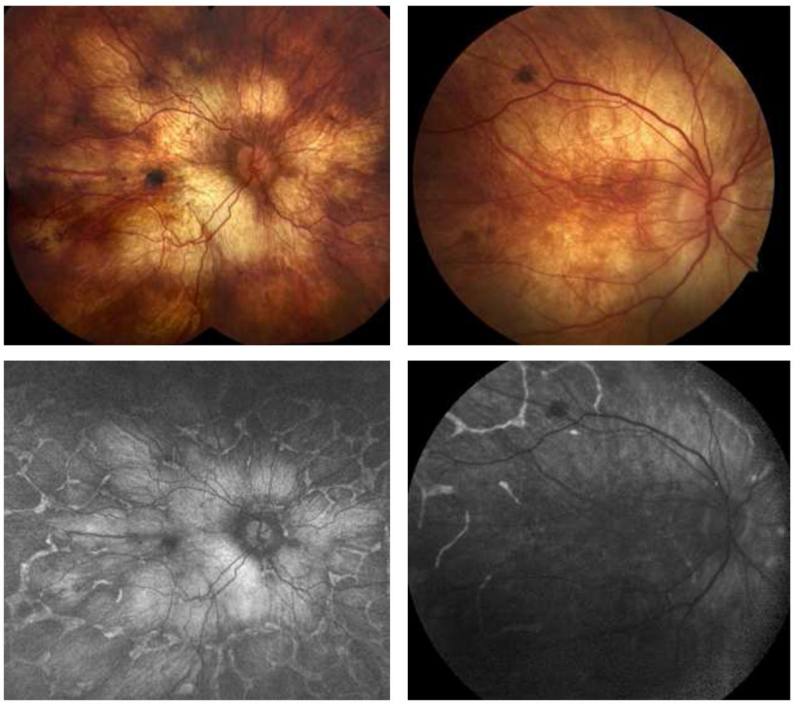

Figure 5. Widefield autofluorescence imaging demonstrates extensive RPE loss that is worst in the posterior pole corresponding to areas of atrophy

(A) Montage of color fundus photographs demonstrating patchy RPE atrophy extending beyond the mid-periphery of two patients (LC03 and LC14) with advanced LCHADD. (B) Corresponding widefield fundus autofluorescence images from the same patients from the same year (LC03) and three years later (LC14) demonstrating extensive RPE loss in the posterior pole. There is a network of residual RPE hyperautofluorescence around well-demarcated nummular regions of RPE loss in the periphery. The diffusely bright signal in areas of RPE loss is thought to be most consistent with scleral autofluorescence, but may represent artifact from wavelength overlap between exciting and detected light.

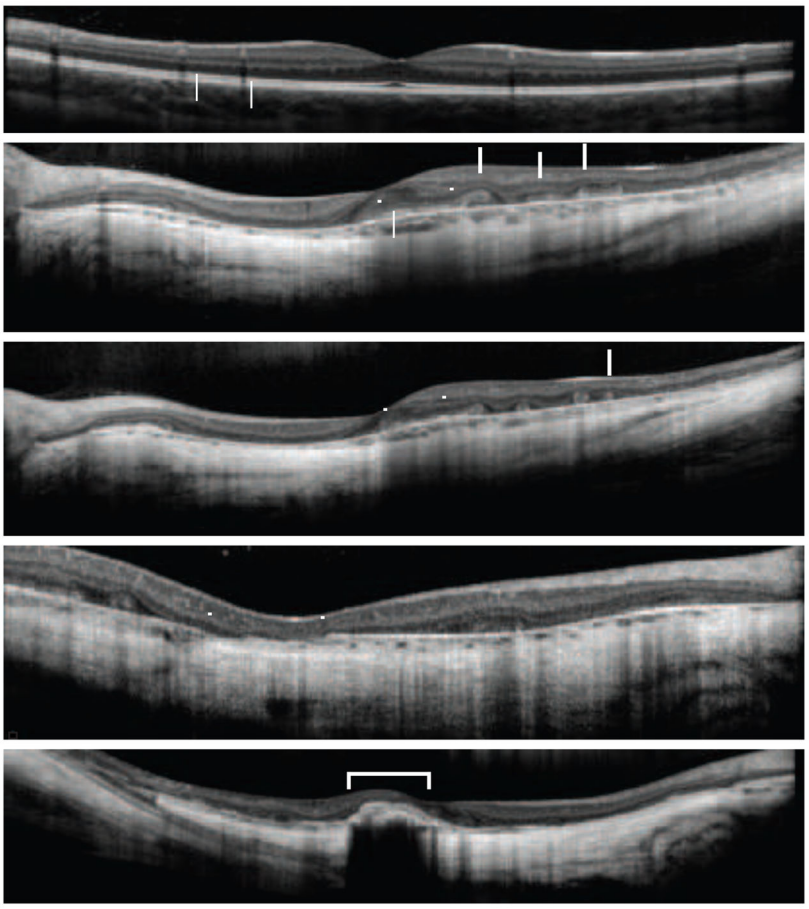

Figure 6. OCT demonstrates progressive atrophy in LCHADD with abrupt transition zones and outer retinal tubulations

(A) Early disease shows mild irregularity of the interdigitation zone (IZ). (B) Ellipsoid zone (EZ) and RPE loss in later stages is characterized by abrupt transition zones [inverted triangles] with scrolling of outer retinal elements and outer retinal tubulations at the margins of degeneration [arrows]. (C) Same eye as in (*B)* 5 years later demonstrates progressive outer retinal atrophy approaching the fovea [inverted triangles] and additional outer retinal tubulation formation [arrows]. (D) Some eyes have apparent breaks in Bruch's membrane [inverted triangles] and (E) subfoveal hyperpigmented scars [bracket] suggestive of a prior CNVM. Nearly all patients had foveal EZ sparing in at least one eye.

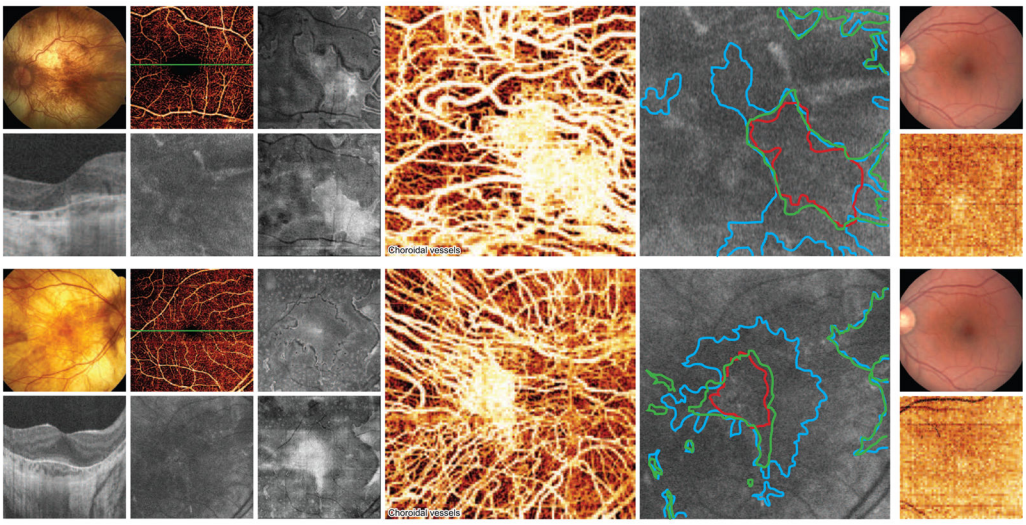

Figure 7. *En face* imaging with OCT angiography suggests the RPE and choriocapillaris loss precede EZ loss in LCHADD

(A–H) LC14, (I–J) 3×3mm control, (K–R) LC25, (S–T) 6×6mm control. (A, K) Color fundus photo outlining the 3×3 mm and 6×6mm locations of the OCT angiography scans respectively. (D, N) OCT cross-section through the fovea as shown on retinal vessel OCT angiogram (B, L). (E, O) Corresponding 3×3mm and 6×6mm autofluorescence images, respectively. (C, M) *En face* OCT slab of the EZ within the outer retina. (F, P) *En face* OCT slab of the RPE. (G, Q) Choroidal OCT angiogram demonstrating a small area of preserved choriocapillaris; surrounding choriocapillaris atrophy results in direct visualization of underlying larger choroidal vessels. (H, R) Overlay of EZ (blue, from C, M), choriocapillaris (red, from G, Q), and RPE (green, from F, P) margins on autofluorescence image. (J, T) OCT choroidal angiography images for a control retina for 3×3mm and 6×6mm scanning areas respectively (I, S). The density of healthy choriocapillaris in (J, T) masks underlying larger choroidal vessels.

Table 1

Baseline demographics and clinical characteristics.

Identification	Sex	Age at Dx (Years)	Age at Eye Visit (Years)		Years of Follow Up	Clinical Presentation	Variant #1	Variant #2	Residual enzyme activity (nmol/min/mg of protein)		Hx of >1 Episode Rhabdomyolysis
			First Visit	Last Visit					LCHAD	Ketothiolase	
LCHADD											
LC01	M	3 months	4.4	12.5	8.1	hypoketotic hypoglycemia	G1528C	G1528C	11.8	38.6	Y
LC02	F	9 months	1.0	15.8	14.8	hypoketotic hypoglycemia	G1528C	c.274-278del			Y
LC03	F	DOL 3	0.8	5.8	5.0	hypoketotic hypoglycemia	G1528C	G1528C			Y
LC04	F	DOL 1	4.7	14.3	9.7	hypoketotic hypoglycemia	G1528C	c.274-278del	10.2	10.7	Y
LC05	M	6 months	9.5	15.8	6.3	hypoketotic hypoglycemia	G1528C	Not Detected			Y
LC06	M	4 months	1.0	7.6	6.6	hypoketotic hypoglycemia	G1528C	G1528C			Y
LC07	F	Birth, dx d/t sibling	2.5	6.4	3.9	none	G1528C	G1528C			Y
LC08	F	4 months	2.1	12.7	10.6	hypoketotic hypoglycemia	G1528C	G1528C	10.7	21.0	Y
LC09	M	5 months	11.1	16.7	5.6	hypoketotic hypoglycemia hypoketotic	G1528C	c.1678C>T			Y
LC10	F	3 months	17.7	18.0	0.3	hypoglycemia, cardiorespiratory arrest	G1528C	G1528C			Y
LC11	F	5 months	0.8	3.3	2.4	hypoketotic hypoglycemia	G1528C	T1678C			lost to f/u
LC12	F	NBS	1.4	5.3	3.8	hypoglycemia	G1528C	Not Detected			Y
LC13	M	6 months	5.6	9.8	4.2	hypoketotic hypoglycemia hypoketotic	G1528C	G1528C			Y
LC14	F	6 months	4.0	24.2	20.2	hypoglycemia, cardiorespiratory arrest	G1528C	c.479-482T AGC>AATA			Y
LC15	M	Birth, dx d/t sibling	0.4	11.3	10.9	none	G1528C	c.274-278del			Y
LC25	F	NBS	11.8	14.2	2.4	none	G1528C	G1528C			Y
LC27	M	Birth, dx d/t family hx	1.6	9.2	7.6	none	G1528C	G1528C			Y
LC31	M	NBS	1.4	5.4	4.0	none	G1528C	splice site mutation (A +3G following exon 3)			N
TFPD											
LC16	F	3 years	10.3	15.5	5.2	rhabdomyolysis	c.901G>A β-subunit	Not Detected			Y
LC17	F	dx d/t sibling	4.7	19.4	14.7	none	c.901G>A β-subunit	Not Detected	12.4	0.4	Y

Identification	Sex	Age at Dx (Years)	Age at Eye Visit (Years)		Years of Follow Up	Clinical Presentation	Variant #1	Variant #2	Residual enzyme activity (nmol/min/mg of protein)		Hx of >1 Episode Rhabdomyolysis
			First Visit	Last Visit					LCHAD	Ketothiolase	
LC18	M	DOL 2	1.0	6.3	5.3	hypoketotic hypoglycemia	c.901G>A β-subunit	Not Detected			Y

NBS=newborn screening. DOL=day of life. Dx=diagnosis. D/t= due to. “Not Detected” indicates that no second mutation was identified.

Table 2

Chorioretinopathy staging at first and last documented exams for each subject demonstrate progression of disease with time.

	Age (Years)	logMAR (OD/OS)	Sph Eq. in Diopters (OD/OS)	Chorioretinopathy Staging (OD/OS)	Age (Years)	logMAR (OD/OS)	Sph Eq. in Diopters (OD/OS)	Chorioretinopathy Staging (OD/OS)
LCHADD								
LC01	6.7	0.54/0.3	−2.75/−2.38	2/2	12.5	0.3/0.3	−6.25/−4.50	3/3
LC02	3.2	CSM/CSM	−1.00/−1.00	2/2	6.8	0.8/1.0	−4.75/−4.88	4/4
LC03	0.8	CSM/CSM	+2.25/+2.25	1*/1*	5.8	0.5/0.3	+0.25/+0.63	2/2
LC04	5.3	0.1/0.1	−0.63/−0.63	2/2*	14.3	1.3/0.3	−5.50/−5.50	4*/4*
LC05	9.5	0.3/0.1	−1.63/−1.00	3/3	15.8	0.3/0.4	−9.50/−8.88	3/*3*
LC06	5.2	0.0/0.0	+1.00/+1.00	2/2	7.6	0.1/0.1	+0.63/+0.50	2/2
LC07	4.0	0.2/0.3	−1.50/−1.50	2/2	6.4	0.2/0.1	−2.00/−2.00	3/3
LC08	8.3	0.4/0.4	−0.50/−0.50	3/3	12.7	0.2/1.0	−8.00/−7.75	4/4
LC09	11.1	−0.1/−0.1	+1.12/+1.94	3/2	14.6	0.0/0.1	−1.88/−0.88	3/3
LC10	17.7	0.9/0.0	−5.13/−5.25	4+*/4+*	18.0	1.0/0.0	−5.13/−5.25	4+*/4+*
LC11	0.8	CSM/CSM	+1.50/+0.75	2*/2*	2.9	CSM/CSM	+1.25/+1.25	2/2
LC12	1.4	CSM/CSM	−0.50/−0.50	2*/2*	5.3	0.0/0.0	−0.75/−1.00	2/2
LC13	7.3	0.6/0.1	0.00/+1.13	2/2	9.8	1.0/0.7	−0.63/0.00	3*/3*
LC14	4.8	0.3/0.3	--	2/2	24.2	1.3/0.1	−3.75/−4.25	4+/4
LC15	0.4	CSM/CSM	−0.88/−0.88	--/--	11.3	0.3/0.4	--	--/--
LC25	11.8	0.2/1.5	−3.23/−4.13	4+*/4*	14.2	0.4/1.4	−3.25/−4.25	4+/4
LC27	1.6	CSM/CSM	--	--/--	9.2	−0.1/0.0	−0.38/−0.13	2*/2*
LC31	1.4	CSM/CSM	+2.50/+2.50	1*/1*	5.4	0.0/0.0	+0.88/+1.00	1*/1*
TFPD								
LC16	10.3	0.1/0.1	+0.93/+1.07	1/1	14.4	0.0/−0.1	0.00/0.00	2/2
LC17	4.7	0.0/0.0	+0.63/+0.68	1/1	8.7	0.0/0.0	+0.38/+0.38	1/1
LC18	1.0	CSM/CSM	+0.75/+1.00	2/2	3.0	CSM/CSM	+0.25/+0.25	2/2

Exam descriptions and fundus photos were used to stage the chorioretinopathy using the fundus staging criteria developed by Tyni et al.[12] The asterisk denotes visits when no fundus photo was available; in these cases, grading was based solely on clinical data. The stage “4+” is not included within Tyni et al. staging criteria, but included to designate times when foveal scarring was appreciated on exam. Corresponding ages, visual acuity (logMAR), spherical equivalent (Sph. Eq.) were included for visits if available. Subject LC15 did not have fundus photos or exam descriptions available to stage. “—“ = unavailable data; “CSM”= central, steady, and maintained.